

Super-Planckian Near-Field Thermal Emission with Phonon-Polaritonic Hyperbolic Metamaterials

S.-A. Biehs and M. Tschikin

Institut für Physik, Carl von Ossietzky Universität, D-26111 Oldenburg, Germany.

R. Messina and P. Ben-Abdallah

Laboratoire Charles Fabry, UMR 8501,

Institut d'Optique, CNRS, Université Paris-Sud 11, 2,

Avenue Augustin Fresnel, 91127 Palaiseau Cedex, France.

(Dated: June 29, 2018)

We study super-Planckian near-field heat exchanges for multilayer hyperbolic metamaterials using exact S-matrix calculations. We investigate heat exchanges between two multilayer hyperbolic metamaterial structures. We show that the super-Planckian emission of such metamaterials can either come from the presence of surface phonon-polaritons modes or from a continuum of hyperbolic modes depending on the choice of composite materials as well as the structural configuration.

In the last few years several fascinating experiments have demonstrated that for small separation distances compared with the thermal wavelength the thermal radiation exchanged between two hot bodies out of thermal equilibrium increases dramatically compared with what we observe at large distances and can even exceed the well-known Stefan-Boltzmann law by orders of magnitude¹⁻⁶. Accordingly, thermal emission is in that case also called super-Planckian emission emphasizing the possibility to go beyond the classical black-body theory. There are several promising applications of super-Planckian emitters ranging from thermal imaging⁷⁻⁹ and thermal rectification/management¹⁰⁻¹² to near-field thermophotovoltaics¹³⁻¹⁷. This has triggered many studies on the possibilities of tailoring and controlling the super-Planckian radiation spectrum by means of designing the material properties¹⁸⁻²³, using phase-change materials²⁴ or 2D systems such as graphene^{25,26}, for instance.

Recently, it was shown that hyperbolic metamaterials can lead to broad-band photonic thermal conductance inside the material itself²⁷ and between two hyperbolic materials only separated by a vacuum gap²⁸. Further Nefedov *et al.* considered nanorod-like structures

made of nanotubes which are interlocked and highlighted a giant radiative heat flux which could be utilized for near-field thermophotovoltaics energy conversion²⁹. Finally, Guo *et al.* have studied the energy density produced by the thermally fluctuating fields close to a hyperbolic structure and found a broadband near-field contribution from which they have concluded that super-Planckian emission will be broad-band for hyperbolic materials³⁰. This is in accordance with the findings in Ref.²⁸ for the energy exchange between two hyperbolic nanowire structures.

The aim of this letter is to show that the surface modes supported by the topmost layers of phonon-polaritonic metamaterials can give the dominant contribution to the super-Planckian emission. As was shown in Ref.³¹ materials which have a broad hyperbolic frequency band as predicted from effective medium theory can support surface modes inside these frequency bands as well which will compete with the hyperbolic modes^{31,32}. In particular, we will show that for the realization of a hyperbolic metamaterial as studied in Ref.³⁰ the main contribution to super-Planckian radiation is not necessarily due to hyperbolic modes but can be due to surface modes depending on the choice of the topmost layer. We will show that in order to allow for broad-band super-Planckian emission by hyperbolic modes, mainly, it is important to use a material for that topmost layer which does not support surface modes in the thermal frequency range.

Before we start to study the super-Planckian thermal radiation let us first recall the concept of indefinite or hyperbolic materials³³⁻³⁵. Such materials are first of all a special class of uni-axial anisotropic materials. For uni-axial materials the permittivity ϵ_{\parallel} parallel to the optical axis is different from the permittivity ϵ_{\perp} perpendicular to the optical axis. For hyperbolic materials one can find frequency bands where ϵ_{\parallel} and ϵ_{\perp} have different signs, i.e. $\epsilon_{\perp}\epsilon_{\parallel} < 0$. Thus the dispersion relation of the photons in such a material³⁶

$$\frac{\kappa^2}{\epsilon_{\perp}} + \frac{k_z^2}{\epsilon_{\parallel}} = \frac{\omega^2}{c^2} \quad (1)$$

describes a hyperbolic function rather than an ellipse as for usual anisotropic materials; here κ (k_z) is the wavevector inside the hyperbolic medium perpendicular (parallel) to the optical axis which is assumed to point in z -direction. Such metamaterials can for example be designed by multilayer structures, since in the long wavelength regime such structures

can be described as homogeneous anisotropic media with the effective permittivities

$$\epsilon_{\perp} = \epsilon_1 f + \epsilon_2 (1 - f), \quad (2)$$

$$\epsilon_{\parallel} = \frac{1}{f/\epsilon_1 + (1 - f)/\epsilon_2}, \quad (3)$$

where ϵ_1 and ϵ_2 are the permittivities of the two layer-materials and f is the filling fraction of the topmost material 1, i.e. $f = l_1/(l_1 + l_2)$. The effective permittivities allow for a calculation of the hyperbolic frequency bands of the multilayer structure where $\epsilon_{\perp}\epsilon_{\parallel} < 0$. There are in general two different kinds of bands: a frequency band Δ_1 where $\epsilon_{\parallel} < 0$ and $\epsilon_{\perp} > 0$ and a frequency band Δ_2 where $\epsilon_{\parallel} > 0$ and $\epsilon_{\perp} < 0$. As will become clear in the following the such calculated frequency bands Δ_1 and Δ_2 can also support surface modes, which are not taken into account in the effective description³¹.

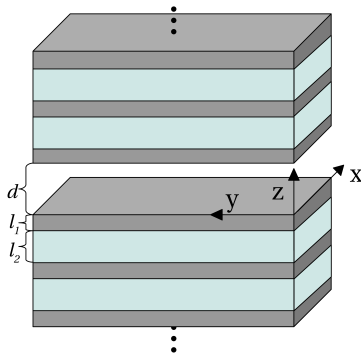


Figure 1: Sketch of the geometry of two hyperbolic multilayer materials separated by a vacuum gap.

In order to study super-Planckian radiation we consider the geometry depicted in Fig. 1. The heat transfer coefficient $h(d)$ between the two metamaterials which are assumed to be at local thermal equilibrium can be determined by³⁷

$$h(d) = \int_0^{\infty} \frac{d\omega}{2\pi} f(\omega, T) \sum_{j=s,p} \int \frac{d^2\kappa}{(2\pi)^2} \mathcal{T}_j(\omega, \kappa; d) = \int_0^{\infty} \frac{d\omega}{2\pi} f(\omega, T) H(\omega, d) \quad (4)$$

where $f(\omega, T) = (\hbar\omega)^2 / (k_B T^2) e^{\hbar\omega/k_B T} / (e^{\hbar\omega/k_B T} - 1)^2$. $\mathcal{T}_s(\omega, \kappa; d)$ and $\mathcal{T}_p(\omega, \kappa; d)$ are the energy transmission coefficients for the s- and p-polarized modes which can be easily determined for semi-infinite materials, anisotropic materials and multilayer structures^{19,38-47}. Here we use the standard S-matrix approach as in Refs.^{42,45} to calculate the amplitude reflection coefficients r_j of our multilayer structures from which we can easily determine the

energy transmission coefficients

$$\mathcal{T}_j(\omega, \kappa; d) = \begin{cases} (1 - |r_j|^2)^2 / |D_j|^2, & \kappa < \omega/c \\ 4[\text{Im}(r_j)]^2 e^{-2|k_{z0}|d} / |D_j|^2, & \kappa > \omega/c \end{cases} \quad (5)$$

including the contributions of the propagating modes with $\kappa < \omega/c$ and the evanescent modes with $\kappa > \omega/c$. Here $D_j = 1 - r_j r_j e^{2ik_{z0}d}$ is a Fabry-Pérot-like denominator with $k_{z0}^2 = k_0^2 - \kappa^2$; $k_0 = \omega/c$.

Now, let us consider a concrete example of a hyperbolic structure which is composed by layers of polar materials. Because these structures can support surface phonon-polaritons as well, they are also called phonon-polaritonic hyperbolic structures. We choose to consider the structure in Ref.³⁰ which is made of layers of SiC and SiO₂. In general amorphous SiO₂ supports surface modes in the infrared as well as SiC, but to get results which are comparable with the calculations done in Ref.³⁰ we assume that $\epsilon_{\text{SiO}_2} = 3.9$ adding a vanishingly small absorption. The optical properties of SiC are taken from Ref.⁴⁸. The layer thicknesses are (a) $l_1 = 50$ nm for the SiC layers and $l_2 = 150$ nm for the silica layers so that the filling fraction is $f = 0.25$ and (b) $l_1 = l_2 = 100$ nm so that $f = 0.5$. For our exact S-matrix calculations we use $N = 50$ where the last layer is a semi-infinite layer with the material properties of the topmost layer. The hyperbolic frequency bands calculated from Eqs. (2) and (3) are (a) $\Delta_1 = 1.495 - 1.623 \cdot 10^{14}$ rad/s and $\Delta_2 = 1.778 - 1.826 \cdot 10^{14}$ rad/s and (b) $\Delta_1 = 1.495 - 1.712 \cdot 10^{14}$ rad/s and $\Delta_2 = 1.712 - 1.827 \cdot 10^{14}$ rad/s.

In order to see the structure of contributing modes we have plotted the transmission coefficient $\mathcal{T}_p(\omega, \kappa; d)$ in Fig. 2. The horizontal dashed white lines mark the hyperbolic bands as determined from effective medium theory³⁶. The solid white lines are the borders of the Bloch bands as determined from Bloch mode dispersion relation for p polarization³⁶

$$\begin{aligned} \cos(k_{z,B}(l_1 + l_2)) = & -\frac{1}{2} \left(\frac{\epsilon_2 k_{z1}}{\epsilon_1 k_{z2}} + \frac{\epsilon_1 k_{z2}}{\epsilon_2 k_{z1}} \right) \sin(k_{z1}l_1) \sin(k_{z2}l_2) \\ & + \cos(k_{z1}l_1) \cos(k_{z2}l_2), \end{aligned} \quad (6)$$

with the permittivities ϵ_i ($i = 1, 2$) of the two layer materials and the wavevector along the optical axis in z direction $k_{zi} = \sqrt{k_0^2 \epsilon_i - \kappa^2}$. Note that $k_{z,B}$ is the Bloch wavevector inside the multilayer structure which can be approximated by its homogenized version k_z in Eq. (1) together with Eqs. (2) and (3) in the regime where the effective description is valid. Only inside these Bloch bands one can find modes which are propagating modes inside the

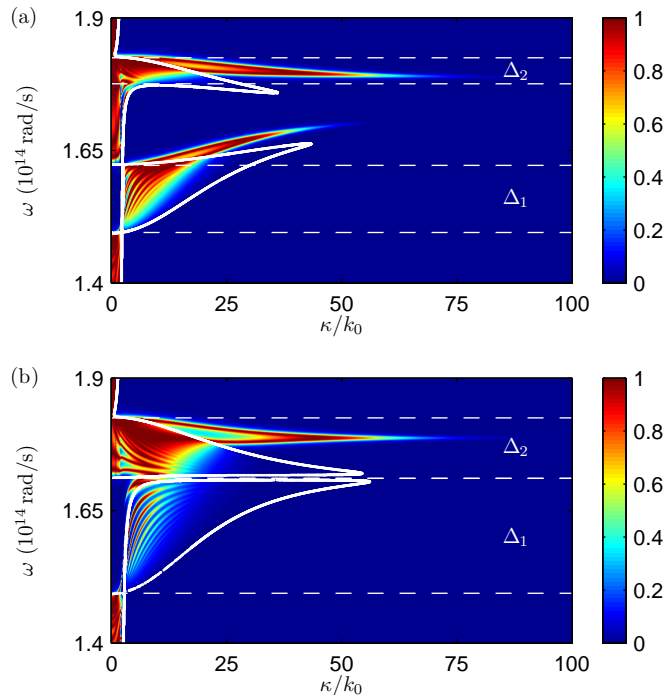


Figure 2: Transmission coefficient $\mathcal{T}_p(\omega, \kappa; d)$ from Eq. (5) for both SiC-SiO₂ multilayer structures (a) $l_1 = 50$ nm and $l_2 = 150$ nm, and (b) $l_1 = l_2 = 100$ nm for the interplate distance $d = 100$ nm.

hyperbolic material. It can be seen that there are also very dominant modes outside the Bloch bands contributing significantly to the energy transmission. These modes are the coupled surface modes of the topmost SiC layers of each hyperbolic material which means that they are evanescent modes inside and outside the hyperbolic structure.

The respective contribution of the modes inside and outside the Bloch bands to the spectral heat transfer coefficient $H(\omega, d)$ is plotted in Fig. 3 for a distance of $d = 100$ nm. From that figure it becomes apparent that within the hyperbolic frequency bands one has quite large contributions stemming from modes outside the Bloch bands which are mainly the coupled surface modes of the topmost layers. Hence, for the chosen structure the broadband super-Planckian radiation from the hyperbolic frequency band is not due to hyperbolic modes only. The relative contribution of surface modes and all the other modes is plotted in Fig. 4 where we show the heat transfer coefficient as a function of distance. From that figure it becomes obvious that for distances about 100 nm and smaller the heat flux is dominated solely by the coupled surface modes of the topmost layers showing a typical $1/d^2$ dependence^{37,49}. Whereas for larger distances the heat flux is dominated by the contributions

inside the Bloch bands. These contributions are on the one hand hyperbolic modes stemming from frequencies inside the hyperbolic bands Δ_1 and Δ_2 . On the other, for frequencies outside the frequency bands Δ_1 and Δ_2 the modes are usual propagating or frustrated total internal reflection modes. Note that for distances of the order of $\max(l_1, l_2)/\pi$ the Bloch-mode contribution reaches a maximum. This can be attributed to the large wavevector cutoff by the edge of the Bloch bands which can be understood as the inset of nonlocal effects since for such distances the main wavevector contributions to the thermal emission are of the order π/d .

To quantify the heat flux mediated by the hyperbolic modes we plot in Fig. 5 the different contributions of the modes inside and outside the Bloch bands, and the contribution from the hyperbolic modes separately. The separate contributions $h_B(d)$, $h_{NB}(d)$, and $h_{hm}(d)$ to the heat transfer coefficient are normalized to the total heat transfer coefficient $h_{tot}(d) = h_B(d) + h_{NB}(d)$. Apparently, in both configurations the contribution of the hyperbolic modes is for all chosen distances smaller than 35%. This is a rather small value for a hyperbolic structure which is constructed for the purpose of enhancing the thermal radiation by the hyperbolic-mode contribution.

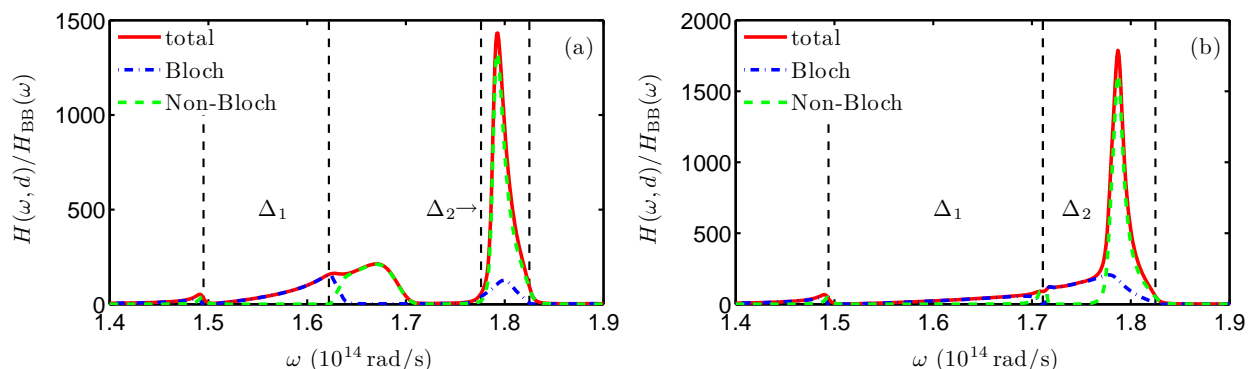


Figure 3: Spectral heat transfer coefficient $H(\omega, d)$ defined in Eq. (4) normalized to the black-body result $H_{BB}(\omega) = \omega^2/(2\pi c^2)$ for both SiC-SiO₂ multilayer structures (a) $l_1 = 50$ nm and $l_2 = 150$ nm, and (b) $l_1 = l_2 = 100$ nm for the interplate distance $d = 100$ nm. Here we choose $T = 300$ K. The vertical dashed lines mark the borders of the hyperbolic frequency bands Δ_1 and Δ_2 .

Now, let us see if the dominant surface-mode contribution vanishes when choosing the passive SiO₂-layer as the topmost layer. Here, it is important to keep in mind that SiO₂ supports surface modes in the infrared. We assume here that it can be described by a

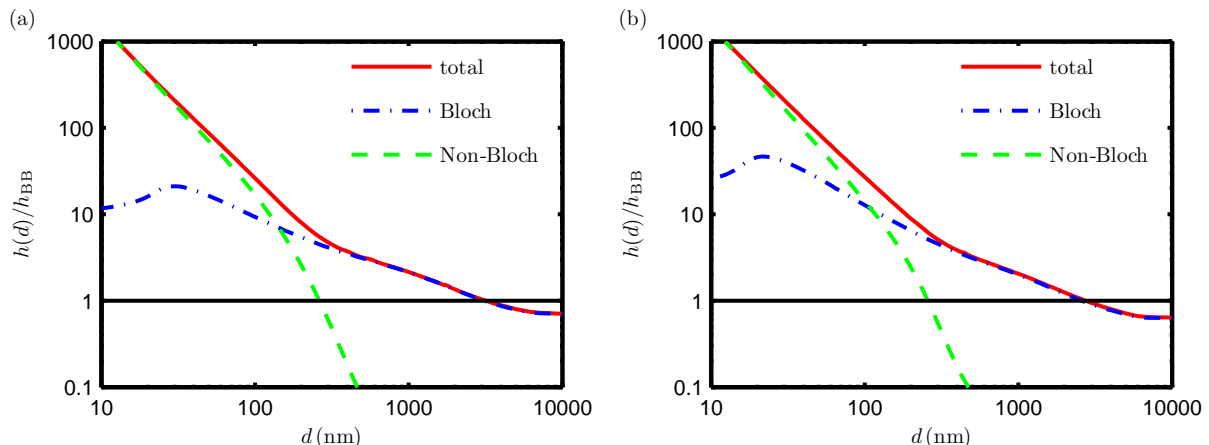


Figure 4: Heat transfer coefficient $h(d)$ from Eq. (4) as a function of interplate distance d using $T = 300$ K for both SiC-SiO₂ multilayer structures (a) $l_1 = 50$ nm and $l_2 = 150$ nm, and (b) $l_1 = l_2 = 100$ nm. The heat transfer coefficient is normalized to the black-body value $h_{\text{BB}} = 6.1 \text{ Wm}^{-2}\text{K}^{-1}$. The contributions from the Bloch bands and from regions outside the Bloch bands are shown separately.

constant permittivity in the frequency band of interest (it is in this sense "passive") in order to compare our results to existing results in the literature. Hence, we repeat the same calculations for the same structure as before but with the difference that for both hyperbolic structures the topmost layer is SiO₂ followed by SiC, etc. The results for the spectral heat transfer coefficient are shown in Fig. 6 (a). There is still a surface-mode contribution, but it is very small compared to the Bloch-mode contributions. Finally, from the distance dependent results in Fig. 6 (b) and (c) it can be seen that the super-Planckian radiation is mainly due to Bloch modes, i.e. frustrated total internal reflection modes and hyperbolic modes. In particular, the contribution of the hyperbolic modes can be larger than 50% in the strong near-field regime for distances of about 10 nm.

As is obvious from Fig. 6 (b) the overall heat flux is only one order of magnitude larger than that of a black body so that the hyperbolic material considered here and in Ref.³⁰ is a poor near-field emitter compared to the previous structures with SiC as topmost layer. But there is a simple method for increasing the hyperbolic contribution by just making the thickness of the layers smaller. Then, the border of the Bloch bands will shift to larger wavevectors which results in a broadband contribution to the transmission coefficient for larger wavevectors and hence to a larger thermal radiation. In Fig. 7 we show the heat

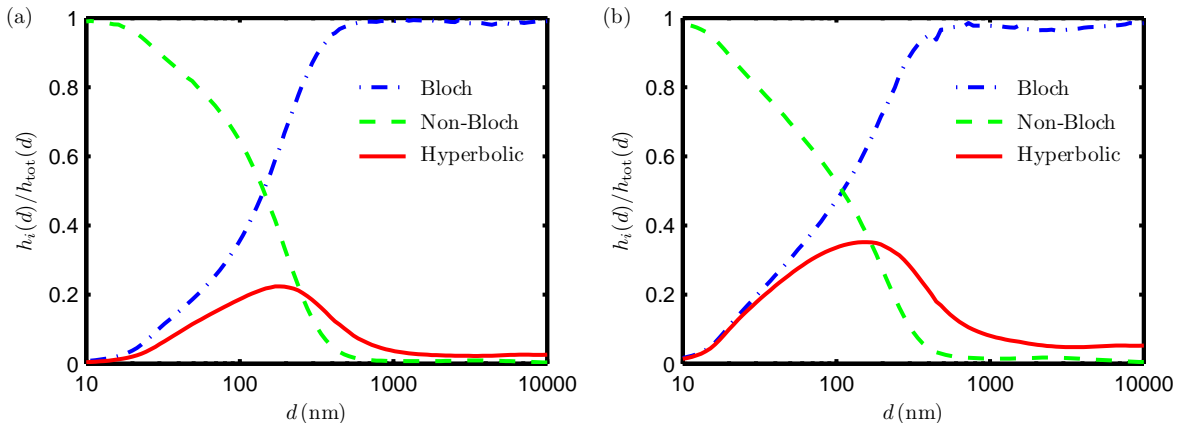


Figure 5: Heat transfer coefficients h_B , h_{NB} , and h_{hm} of the Bloch modes, the modes outside the Bloch bands and the hyperbolic modes normalized to the total heat transfer coefficient $h_{tot}(d) = h_B(d) + h_{NB}(d)$ as a function of distance. Again we show both cases (a) $l_1 = 50$ nm and $l_2 = 150$ nm, and (b) $l_1 = l_2 = 100$ nm, and set $T = 300$ K.

flux for hyperbolic structures with a filling factor of 0.5 but layer thicknesses of 100 nm, 50 nm and 5 nm. It can be seen that the heat flux increases by orders of magnitude in the strong near-field regimes, i.e., for distances smaller than 100 nm, when making the layers thinner. We have checked that the main contribution is due to hyperbolic modes in that regime (not shown here). Further studies have to find an optimized design and optimal composite materials in order to further improve the thermal radiation properties of hyperbolic materials to attain thermal heat fluxes which are as large as the heat flux by surface modes or even larger. Note that in Ref.²⁸ such a structure was proposed on the basis of an effective description.

In conclusion, we have studied the super-Planckian emission of hyperbolic structures by using the fluctuational electrodynamics theory combined with the S-matrix method. It has been shown that to properly describe the energy exchanges it is of crucial importance not only to choose a good combination of material composites for having broad-band super-Planckian radiation but also to use a passive material as topmost layer, i.e. a material which does not support surface mode resonances within the thermally accessible spectrum. Also, we have shown for multilayer structures that the thickness of layers determines the wavevector cutoff of the Bloch band so that it appears clearly advantageous to use thin layers with elementary thicknesses $l_1, l_2 \ll d$ to observe a large super-Planckian emission

at a given distance d from the surface. These findings provide the basis for realizing an optimized design of hyperbolic thermal emitters with broad-band super-Planckian spectra.

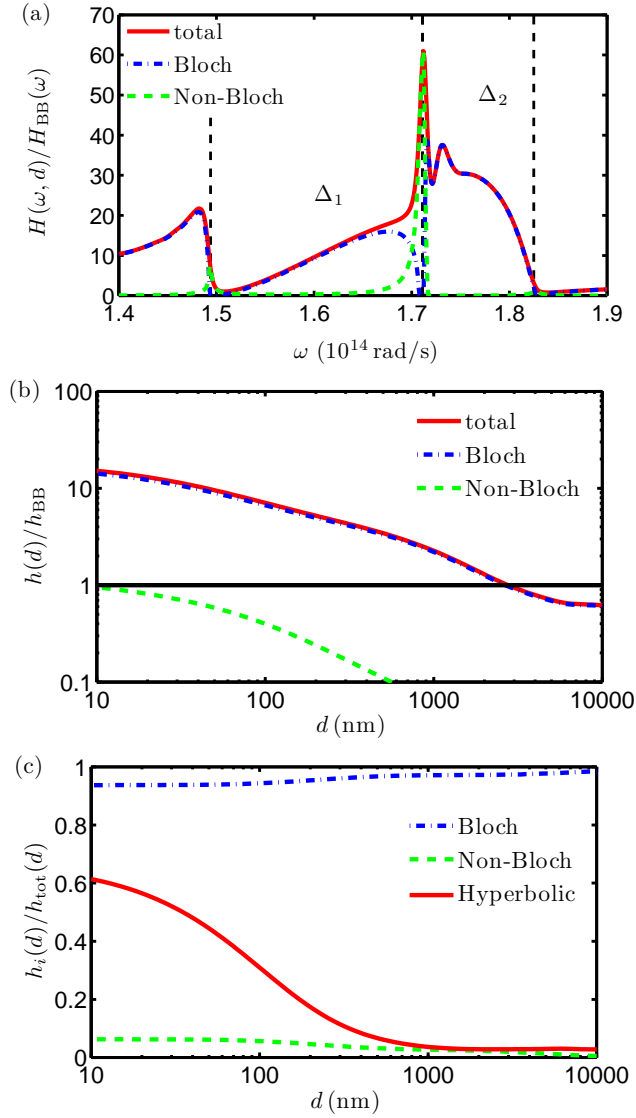


Figure 6: (a) Spectral heat transfer coefficients $H(\omega, d)$ between two hyperbolic materials with SiO_2 as topmost layer choosing $d = 100$ nm. The vertical dashed lines mark the borders of the hyperbolic frequency bands Δ_1 and Δ_2 . (b) Heat transfer coefficients $h(d)$ for the same materials setting $T = 300$ K normalized to the black-body value $h_{\text{BB}} = 6.1 \text{ Wm}^{-2}\text{K}^{-1}$. Finally in (c) we plot the relative contributions of the Bloch modes, Non-Bloch modes and the hyperbolic modes.

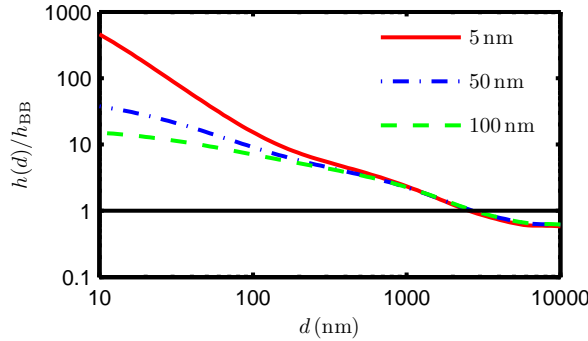


Figure 7: The heat transfer coefficient for the structure with the passive material as topmost layer for different layer thicknesses $l_1 = l_2$ ($f = 0.5$) of 100 nm, 50 nm, and 5 nm normalized to the black-body value $h_{\text{BB}} = 6.1 \text{ Wm}^{-2}\text{K}^{-1}$.

Acknowledgments

M.T. gratefully acknowledges support from the Stiftung der Metallindustrie im Nord-Westen. The authors acknowledge financial support by the DAAD and Partenariat Hubert Curien Procope Program (project 55923991). This work has been partially supported by the Agence Nationale de la Recherche through the Source-TPV project ANR 2010 BLANC 0928 01.

-
- ¹ L. Hu, A. Narayanaswamy, X. Chen, and G. Chen, *Appl. Phys. Lett.* **92**, 133106 (2008).
 - ² A. Narayanaswamy, S. Shen, and G. Chen, *Phys. Rev. B* **78**, 115303 (2008).
 - ³ S. Shen, A. Narayanaswamy, and G. Chen, *Nano Lett.* **9**, 2909 (2009).
 - ⁴ E. Rousseau, A. Siria, G. Jourdan, S. Volz, F. Comin, J. Chevrier and J.-J. Greffet, *Nature Photonics* **3**, 514 (2009).
 - ⁵ R. S. Ottens, V. Quetschke, S. Wise, A. A. Alemi, R. Lundock, G. Mueller, D. H. Reitze, D. B. Tanner, and B. F. Whiting, *Phys. Rev. Lett.* **107**, 014301 (2011).
 - ⁶ T. Kralik, P. Hanzelka, M. Zobac, V. Musilova, T. Fort, and M. Horak, *Phys. Rev. Lett.* **109**, 224302 (2012).
 - ⁷ Y. De Wilde, F. Formanek, R. Carminati, B. Gralak, P.A. Lemoine, K. Joulain, J.P. Mulet, Y. Chen, and J.J. Greffet, *Nature* **444**, 740 (2006).

- ⁸ A. Kittel , U. Wischnath , J. Welker , O. Huth , F. Rütting, and S.-A. Biehs, *Appl. Phys. Lett.* **93**, 193109 (2008).
- ⁹ F. Huth, M. Schnell, J. Wittborn, N. Ocelic and R. Hillenbrand, *Nature Materials* **10**, 352 (2011).
- ¹⁰ C. R. Otey, W. T. Lau, and S. Fan, *Phys. Rev. Lett.* **104** 154301 (2010).
- ¹¹ S. Basu and M. Francoeur, *Appl. Phys. Lett.* **98**, 113106 (2011).
- ¹² S.-A. Biehs, F. S. S. Rosa, and P. Ben-Abdallah, *Appl. Phys. Lett.* **98**, 243102 (2011).
- ¹³ R. S. DiMatteo, P. Greiff, S. L. Finberg, K. A. Young-Waithe, H. K. Choy, M. M. Masaki, and C. G. Fonstad, *Appl. Phys. Lett.* **79**, 1894 (2001).
- ¹⁴ A. Narayanaswamy and G. Chen, *Appl. Phys. Lett.* **82**, 3544 (2003).
- ¹⁵ M. Laroche, R. Carminati, and J.-J. Greffet, *J. Appl. Phys.* **100**, 063704 (2006).
- ¹⁶ K. Park, S. Basu, W. P. King, and Z. M. Zhang, *J. Quant. Spect. Rad. Transf.* **109**, 305 (2008).
- ¹⁷ S. Basu, Z. M. Zhang, and C. J. Fu, *International Journal of Energy Research* **33**, 1203 (2009).
- ¹⁸ C.J. Fu and Z. M. Zhang, *Int. J. Heat Mass Transfer* **49**, 1703 (2006).
- ¹⁹ S.-A. Biehs, P. Ben-Abdallah, F. S. S. Rosa, K. Joulain, and J.-J. Greffet, *Opt. Expr.* **19**, A1088 (2011).
- ²⁰ K. Joulain, J. Drevillon, and P. Ben-Abdallah, *Phys. Rev. B* **81**, 165119 (2010).
- ²¹ R. Guérout, J. Lussange, F. S. S. Rosa, J.-P. Hugonin, D. A. R. Dalvit, J.-J. Greffet, A. Lambrecht, and S. Reynaud, *Phys. Rev. B* **85** (R), 180301 (2012).
- ²² J. Lussange, R. Guérout, F. S. S. Rosa, J.-J. Greffet, A. Lambrecht, and S. Reynaud, *Phys. Rev. B* **86**, 085432 (2012).
- ²³ L. Cui, Y. Huang, J. Wang, and K.-Y. Zhu, *Appl. Phys. Lett.* **102**, 053106 (2013).
- ²⁴ P. J. van Zwol, K. Joulain, P. Ben-Abdallah, and J. Chevrier, *Phys. Rev. B* **84**, 161413 (2011).
- ²⁵ V. B. Svetovoy, P. J. van Zwol, and J. Chevrier, *Phys. Rev. B* **85**, 155418 (2012).
- ²⁶ O. Ilic, M. Jablan, J. D. Joannopoulos, I. Celanovic, H. Buljan, and M. Soljačić, *Phys. Rev. B* **85**, 155422 (2012).
- ²⁷ E. E. Narimanov and I. I. Smolyaninov, arXiv:1109.5444v1.
- ²⁸ S.-A. Biehs, M. Tschikin, and P. Ben-Abdallah, *Phys. Rev. Lett.* **109**, 104301 (2012).
- ²⁹ I. S. Nefedov and C. R. Simovski, *Phys. Rev. B* **84**, 195459 (2011).
- ³⁰ Y. Guo, C. L. Cortes, S. Molesky, and Z. Jacob, *Appl. Phys. Lett.* **101**, 131106 (2012).
- ³¹ M. Tschikin, S.-A. Biehs, R. Messina, and P. Ben-Abdallah, submitted (2012).

- ³² G. Rosenblatt and M. Orenstein, *Opt. Exp.* **19**, 20372 (2011).
- ³³ D. R. Smith, Willie J. Padilla, D. C. Vier, S. C. Nemat-Nasser and S. Schultz, *Phys. Rev. Lett.* **84**, 4184 (2000).
- ³⁴ D. R. Smith and D. Schurig, *Phys. Rev. Lett.* **90**, 077405 (2003).
- ³⁵ L. Hu and S. T. Chui, *Phys. Rev. B* **66**, 085108 (2002).
- ³⁶ P. Yeh, *Optical Waves in Layered Media*, (Wiley, Hoboken, 2005).
- ³⁷ K. Joulain, J.-P. Mulet, F. Marquier, R. Carminati, and J.-J. Greffet, *Surf. Sci. Rep.* **57**, 59-112 (2005).
- ³⁸ S.-A. Biehs, *Eur. Phys. J. B* **58**, 423 (2007).
- ³⁹ M. Francoeur, P. Mengüç, and R. Vaillon, *Appl. Phys. Lett.* **93**, 043109 (2008).
- ⁴⁰ W. T. Lau, J.-T. Shen, G. Veronis, S. Fan, and P. V. Braun, *Appl. Phys. Lett.* **92**, 103106 (2008); W. T. Lau, J.-T. Shen, and S. Fan, *Phys. Rev. B* **80**, 155135 (2009).
- ⁴¹ P. Ben-Abdallah, K. Joulain, J. Drevillon, and G. Domingues, *J. Appl. Phys.* **106**, 044306 (2009).
- ⁴² M. Francoeur, P. Mengüç, R. Vaillon, *J. Quant. Spect. Rad. Transf.* **110**, 2002 (2009).
- ⁴³ P. Ben-Abdallah, K. Joulain, and A. Pryamikov., *Appl. Phys. Lett* **96**, 143117 (2010).
- ⁴⁴ A. Pryamikov, K. Joulain, P. Ben-Abdallah, J. Drevillon, *J. Quant. Spect. Rad.* **112**, 1314 (2011).
- ⁴⁵ M. Tschikin, P. Ben-Abdallah and Svend-Age Biehs, *Phys. Lett. A* **376**, 3462 (2012).
- ⁴⁶ R. Messina, M. Antezza, P. Ben-Abdallah, *Phys. Rev. Lett.* **109**, 244302 (2012).
- ⁴⁷ S. I. Maslovski, C. R. Simovski, S. A. Tretyakov, arXiv:1210.6569v1.
- ⁴⁸ E. D. Palik, *Handbook of Optical Constants of Solids*, (Academic Press, Florida, 1985).
- ⁴⁹ A. I. Volokitin and B. N. J. Persson, *Rev. Mod. Phys.* **79**, 1291 (2007).

